First-principles study of interaction of cluster Au_{32} with CO, H_2, and O_2

Yao Wang
Key Laboratory of Materials Physics, Institute of Solid State Physics, Chinese Academy of Sciences, Hefei 230031, China

X. G. Gong[a)]
Surface Physics Laboratory and Department of Physics, Fudan University, Shanghai 200433, China

(Received 13 February 2006; accepted 14 August 2006; published online 22 September 2006)

First-principles calculations are performed to study the interaction of cluster Au_{32} with small molecules, such as CO, H_2, and O_2. The cagelike $Au_{32}(I_h)$ shows a higher chemical inertness than the amorphous $Au_{32}(C_1)$ with respect to the interaction with small molecules CO, H_2, and O_2. H_2 can only be physically adsorbed on $Au_{32}(I_h)$, while it can be dissociatively chemisorbed on $Au_{32}(C_1)$. Although CO can be chemically adsorbed on $Au_{32}(I_h)$ and $Au_{32}(C_1)$ with one electron transferred from Au_{32} to the antibonding π^* orbit of CO, it is bound more strongly on $Au_{32}(C_1)$ than on $Au_{32}(I_h)$. Spin polarized and spin nonpolarized calculations result almost identical ground state structures of $Au_{32}(I_h)-O_2$ and $Au_{32}(C_1)-O_2$, in which O_2 is dissociatively chemisorbed. © *2006 American Institute of Physics*. [DOI: 10.1063/1.2352749]

I. INTRODUCTION

Nanosized gold clusters have attracted much attention from both industrial and scientific areas due to their unique physical and chemical properties strongly dependent on the cluster size.[1,2] Although bulk Au is one of the most chemically inert metals, small Au clusters, the size of which is as small as 2–3 nm, are efficient catalysts for various chemical reactions.[3,4] Previous studies reported that nanosized Au catalysts could be applied to many oxidation and hydrogenation reactions at low temperatures. These reactions include CO and NO oxidations,[5] partial oxidation of propylene,[6] partial hydrogenation of acetylene,[7] and hydrogenations of ethylene, 1,3-butadiene, 1-butene,[8] acrolein,[9] and so on. However, up to now, the mechanism of such fantastic size-dependent catalytic activity of Au clusters has not been clearly revealed. Therefore, Au clusters and the interactions of Au clusters with small molecules, such as O_2, H_2, CO, NO, and CH_4, have become hot topics in both experimental and theoretical fields.

The interactions of Au clusters with small molecules have been extensively studied. Previous studies found that the interaction behaviors of small molecules with Au clusters were dependent on the size and structural properties of the clusters. For the interaction of Au clusters with O_2, it was experimentally found that an odd-even alteration as a function of the number of Au atoms of the cluster exhibited in the interaction between Au_n^- ($n<22$) and O_2 molecules: one O_2 could be strongly adsorbed on Au_n^- (n=even); whereas for Au_n^- (n=odd), no adsorption of O_2 except only very weak reaction with O_2 was observed. Meanwhile no O_2 adsorption was observed on Au_n^- ($20<n<27$), Au_n, and Au_n^+, except Au_{10}^+.[10–14] The experimental studies, especially those focused on the interaction properties between O_2 and the Au_n^- of even atoms up to Au_{20}^-, found the nondissociative chemisorption of O_2 at room temperature.[15] Results of the first principles calculations were in agreement with experimental observations, although some discrepancies existed between them. For example, the odd-even alteration, as a function of the number of Au atoms in the interaction of Au clusters with O_2, was also found by theoretical calculations, while the theoretical results of adsorption states of O_2 (molecular adsorption or dissociative adsorption) and the number of adsorbed O_2 molecules were not exactly coincident with the experimental results.[16–19] For the interaction of Au clusters with CO, theoretical calculations found that CO was a two-electron donor; therefore, Au_n^+ bound CO more strongly than Au_n and Au_n^-. Moreover the changes of the binding energy of CO adsorbed on Au_n^+ and Au_n^- with the size of gold cluster were different from each other, it decreased for Au_n^+ bit increased for Au_n^-. For all Au clusters, the most favorable adsorption site of CO was the top of the cluster with low coordination sites.[20–23] An experimental study reported that each Au cluster had a critical CO number (nc), exactly equal to the number of the available low-coordination apex sites on this cluster.[24] In addition, both experimental and theoretical studies revealed that O_2 and CO were able to be coadsorbed on Au clusters, because the adsorption of one kind of molecule favored that of another kind of molecule. Meanwhile the coadsorption could induce the oxidation of CO, i.e., Au clusters behaved as a catalyst facilitating the oxidation of CO.[25–29] The studies of the interaction of Au clusters with H_2 were relatively rare. Early experiment reported that the reaction of Au_n^+ with H_2 might be observed under high pressure and temperature conditions; recent experiments found no reactivity of Au_n^+ toward H_2 under usual experimental condition, because the binding between Au_n^+ and H_2 was weak and the reaction of Au_n^+ with H_2 needed to overcome a high barrier.[10,30] A theoretical study found that H_2 could be molecularly bound to Au_2 and Au_3, but could not be bound to Au_2^- and Au_3^-.[31] Besides, the gas-phase Au clusters, Au clus-

[a)]Electronic mail: xggong@fudan.edu.cn

ters supported by metal oxides, have also been extensively studied. Recently, joint experimental and theoretical studies on Au_n $(2 \leqslant n \leqslant 20)$ supported by MgO surface revealed that Au_8 was the smallest gold heterogeneous catalyst for the oxidation of CO. It was reported that when Au_8 was bound to oxygen vacancy F centers of MgO surface, it was catalytically active; while it was catalytically inert when bound to MgO defect-free surface.[32] Some theoretical studies found that oxide enhanced the catalytic activity of Au clusters.[33,34] Meanwhile it was found experimentally that different oxides showed different effects on the activity of Au clusters: the activity of Au clusters supported by the reducible oxides (TiO_2 and Fe_2O_3) was higher than that supported by irreducible oxides (MgO, Al_2O_3, and SiO_2).[5,35] It was also found experimentally that the lowest temperature, at which TiO_2 supported Au clusters catalyzed the oxidation of CO, was 65 K.[36]

Recent experimental and theoretical studies found that the relativistic effect played a significant role in the structures of small Au clusters, resulting in the structures of Au clusters different from the clusters of other metals. For example, neutral and anionic clusters Au_n and Au_n^- favored planar structure up to $n=13$, cationic cluster Au_n^+ favored planar structure up to $n=8$, while the clusters of five to seven atoms of other metals would transfer to three-dimensional structure.[37,38] The photoelectron spectroscopy combined with the relativistic density functional calculations revealed that Au_{20} possessed a tetrahedral structure with a wide highest occupied molecular orbital-lowest unoccupied molecular orbital (HOMO-LUMO) gap of 1.77 eV. This suggested that Au_{20} should be highly inert and stable. CO favored to be molecularly adsorbed on the apex sites of the Au_{20} tetrahedron and the HOMO-LUMO gap of the tetrahedral Au_{20} was slightly decreased upon CO adsorption.[39] Another x-ray photoelectron spectroscopy showed that Au_{55} supported by silicon substrate presented a maximum oxidation resistance; therefore it might exhibit unusual catalytic properties.[40] Recently, the first-principles calculations have found that clusters Au_n $(n=32-35)$ can appear in cagelike structure with a wide HOMO-LUMO gap. The most typical example is cluster $Au_{32}(I_h)$ of icosahedral symmetry; its gap is as wide as 1.56 eV. This suggested that $Au_{32}(I_h)$ should have a high chemical inertness.[41] Although $Au_{32}(I_h)$ is the most stable one at zero temperature, experimental and theoretical studies have found that its amorphous isomer $Au_{32}(C_1)$ becomes most stable above 300 K.[42]

In this paper, in order to investigate the chemical properties of cluster Au_{32}, first-principles calculations are carried out to compare the interactions of clusters $Au_{32}(I_h)$ and $Au_{32}(C_1)$ with selected small molecules, i.e., CO, H_2, and O_2. It is found that $Au_{32}(I_h)$ shows a high chemical inertness with respect to these interactions.

II. DETAILS OF CALCULATIONS

The present calculations are based on the density functional theory[43,44] and plane-wave basis set[45,46] with generalized gradient approximation (GGA),[47,48] which are implemented in the VASP code.[49] The interaction between core and valence electrons is described with the projector augmented wave (PAW) potential.[50,51] The structures of the clusters are optimized by the conjugate gradient (CG) method.[52] A simple cubic supercell with a lattice constant of 25 Å is adopted, which is large enough to neglect the interaction between the cluster and its periodic images. Due to the large supercell, only Γ point is used for the summation in the Brillouin zone. The structures of $Au_{32}(I_h)$ and $Au_{32}(C_1)$ (see Fig. 1) are first optimized to make them coincident with the previous theoretical studies,[41,42] then the small molecules, i.e., CO, H_2, and O_2, or their atomic forms, such as C, O, and H, are added on. Finally, the structure with the highest binding energy is taken as the ground-state structure. If, for example, the structure with two O atoms separately absorbed on the cluster is of higher binding energy than that of the structure with O_2 molecularly absorbed, we say O_2 can dissociatively adsorb on the cluster, without calculating the exact barrier. In order to test the accuracy of the present method, the bond lengths of Au_2, CO, H_2, and O_2 are calculated. The results are 2.49, 1.14, 0.75, and 1.31 Å, respectively, in agreement with the experimental results of 2.47, 1.13, 0.73, and 1.21 Å.

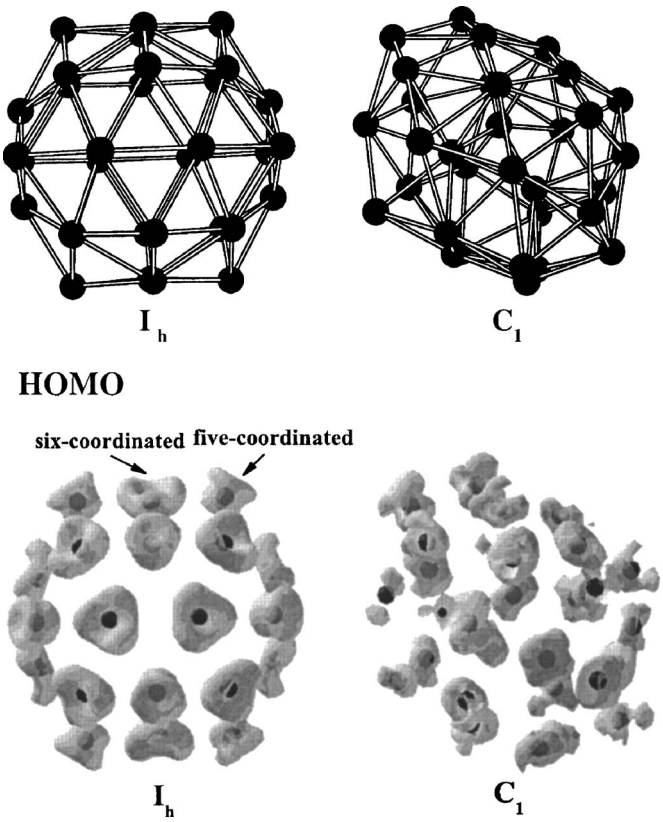

FIG. 1. Structure and highest occupied state (HOMO) of clusters $Au_{32}(I_h)$ and $Au_{32}(C_1)$. The HOMO plots show equal density surface of 0.04 electrons/Å.

III. RESULTS AND DISCUSSIONS

A. Interaction between cluster Au_{32} and CO

For the present calculations, two types of cluster Au_{32} are selected to study the interaction with small molecules: one is $Au_{32}(I_h)$, which is the ground state structure of cluster

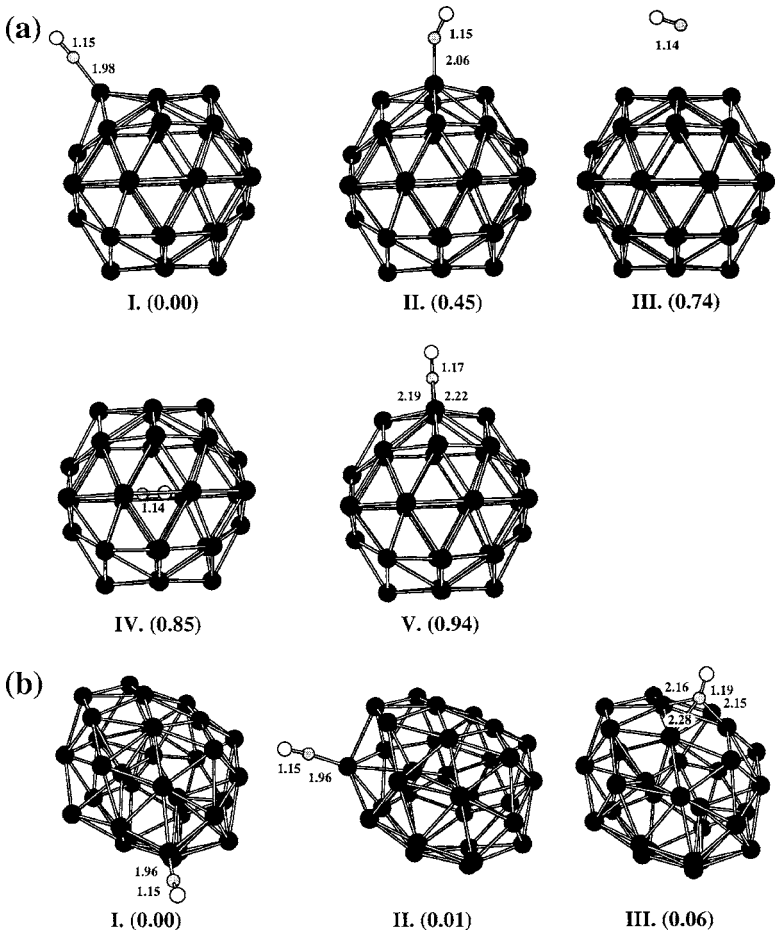

FIG. 2. Structures of Au_{32}–CO: (a) $Au_{32}(I_h)$–CO and (b) $Au_{32}(C_1)$–CO. The gray balls represent C atoms, and the white balls represent O atoms. The bond lengths of C–O and Au–C are given in Å. What shown in the brackets are the relative energies to the total energies of the ground state structures of $Au_{32}(I_h)$–CO and $Au_{32}(C_1)$–CO, respectively, in eV.

Au_{32} at 0 K; and the other is $Au_{32}(C_1)$, which is the most stable structure of cluster Au_{32} above 300 K.[41,42] First, the structural and electronic properties of $Au_{32}(I_h)$ and $Au_{32}(C_1)$ (shown in Fig. 1) are discussed. $Au_{32}(I_h)$ is of high symmetry: there are only two different kinds of site on the cage, i.e., 12 five-coordinated sites and 20 six-coordinated sites. The HOMO charge density of $Au_{32}(I_h)$ is plotted in Fig. 1. It is shown that the HOMO spreads symmetrically over the outer surface of the $Au_{32}(I_h)$ cage: protrudes outwards at the five-coordinated sites and sinks inwards at the six-coordinated sites. Thus, at the five-coordinated sites, the HOMO of $Au_{32}(I_h)$ should overlap with those of other molecules more than at the six-coordinated sites. This means that the atoms at the five-coordinated sites should be more active than those at the six-coordinated sites and small molecules should be adsorbed more favorably on the five-coordinated sites. However, for $Au_{32}(C_1)$, the structure without any symmetry results in the distribution of its HOMO charge density without any symmetry.

In order to study the interaction between cluster Au_{32} and CO, the structures of both $Au_{32}(I_h)$–CO and $Au_{32}(C_1)$–CO complexes are optimized. The structural and electronic properties of Au_{32}–CO complexes are displayed in Figs. 2 and 3 and listed in Table I. Figure 2 shows the optimized structures of $Au_{32}(I_h)$–CO (a) and $Au_{32}(C_1)$–CO (b), while the binding energy of CO, HOMO-LUMO gap, and bond lengths of C–O and Au–C of each complex are listed in Table I. The HOMO charge densities of the isomers of $Au_{32}(I_h)$–CO complex are shown in Fig. 3.

Because of the high symmetry of $Au_{32}(I_h)$, the possible binding sites of CO are very few. Therefore, in the present calculations, only five stable structures of $Au_{32}(I_h)$–CO complex are obtained. All of them are shown in Fig. 2(a). For the first two most stable structures of $Au_{32}(I_h)$–CO [(I) and (II) of Fig. 2(a)], CO molecules are adsorbed on the on-top sites of the $Au_{32}(I_h)$ cage. In the ground state of $Au_{32}(I_h)$–CO [(I) of Fig. 2(a)], CO is adsorbed on the five-coordinated site; while in the first isomer [(II) of Fig. 2(a)], CO is adsorbed on the six-coordinated site. The binding energy of CO of the former is 0.86 eV, while it is 0.40 eV for the latter. This indicates that CO should be adsorbed much more favorably on the five-coordinated sites, the lower-coordinated sites, showing the higher activity of the Au atoms at the five-coordinated sites. This result is in agreement with previous experimental and theoretical studies on the adsorption of CO on small gold clusters: CO ought to prefer to be bound on the low-coordinated sites of small gold clusters.[20–24] Examination on these two most stable structures of $Au_{32}(I_h)$–CO shows that $Au_{32}(I_h)$ cages only change slightly upon CO adsorption. The C atom of CO likes to be bound to one single Au atom with C–O bond length of 1.15 Å, which is equal to that of CO^- and 0.01 Å longer than that of a free CO molecule (1.14 Å). In previous study, the interaction between CO and transition metal surface was generally characterized by the charge transfer from the metal to the antibonding (π^*) orbit of CO (donation) and back donation to the metal from the CO bonding (σ) orbit.[53] The present calculation suggests that for the two most stable

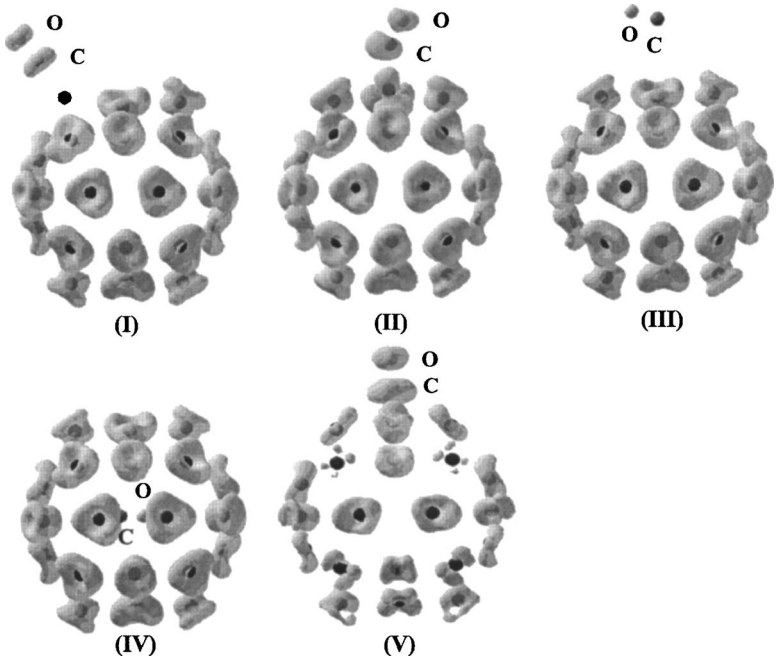

FIG. 3. The highest occupied states (HOMO) of $Au_{32}(I_h)$–CO complexes. The plots show equal density surface of 0.04 electrons/Å.

structures of $Au_{32}(I_h)$–CO one electron might transfer from $Au_{32}(I_h)$ to the π^* orbit of CO, i.e., CO could be chemisorbed on $Au_{32}(I_h)$ cage. The plots of the HOMO charge densities of these two most stable structures are shown in Fig. 3 [(I) and (II)]. It can be clearly seen that CO molecules gain electrons, while the Au atoms, on which CO are bound, lose electrons. The charge transfer from $Au_{32}(I_h)$ to the π^* orbit of CO results in the formation of Au–C bonds. The chemical adsorption of CO leads to a slight decrease of the HOMO-LUMO gap of $Au_{32}(I_h)$ to 1.45 eV for the ground-state structure [(I) in Fig. 2(a)] and 1.26 eV for the first isomer [(II) in Fig. 2(a)]. Comparison of the geometric and electronic properties of the two most stable structures of $Au_{32}(I_h)$–CO with those of cluster $Au_{32}(I_h)$ shows that the influence of CO adsorption on $Au_{32}(I_h)$ is not noticeable.

As for the third stable structure of $Au_{32}(I_h)$–CO [(III) in Fig. 2(a)], CO stays on the outer surface of the $Au_{32}(I_h)$ cage with CO binding energy of 0.12 eV, while for the fourth stable structure of $Au_{32}(I_h)$–CO [(IV) in Fig. 2(a)], CO stays at the inner center of the $Au_{32}(I_h)$ cage, with a much less CO binding energy of 0.01 eV. This means that in these two cases, CO does not strongly interact with $Au_{32}(I_h)$ cages. In fact, CO molecule keeps its free molecule state, with a bond length of 1.14 Å, while the $Au_{32}(I_h)$ cages also keep their original structures unchanged. The HOMO charge densities of these two structures are shown in Fig. 3, which confirm the argument mentioned above: for each case the HOMO keeps the same distribution as a free $Au_{32}(I_h)$ cluster, independent of the CO adsorption. Therefore, in these two structures, neither charge transfer nor bond formation could occur between $Au_{32}(I_h)$ and CO. Meanwhile, the wide HOMO-LUMO gap of the $Au_{32}(I_h)$ cage is also not obviously affected by CO adsorption, it is 1.53 and 1.56 eV for the third and the fourth stable structures, respectively. In comparison, the HOMO-LUMO gap of a free cluster $Au_{32}(I_h)$ is 1.56 eV. Briefly CO adsorption has no noticeable effect on the geometric and electronic structures of the free $Au_{32}(I_h)$ cage. Therefore, it can be concluded that CO can freely stay either on the outer surface or at the inner center of $Au_{32}(I_h)$ cages. This behavior of $Au_{32}(I_h)$ cage is different from that of C_{60} cage which destabilizes the CO staying at its center.[54]

All the above four stable structures of $Au_{32}(I_h)$–CO are formed exothermically. However, the CO binding energy of the fifth structure of $Au_{32}(I_h)$–CO complex [(V) in Fig. 2(a)] is −0.08 eV, which means its formation is endothermic. In this structure, CO stays on the bridge site between two six-coordinated Au atoms. Two Au–C bonds formed with slightly different bond lengths, 2.19 and 2.22 Å, which are longer than the Au–C bonds in the two most stable structures. The adsorption of CO makes $Au_{32}(I_h)$ cage broken; the bond length between the two six-coordinated Au atoms increases to 3.16 Å, 0.3 Å longer than the original bond length, while the bond length of CO increases to 1.17 Å, showing that more than one electron transfer from $Au_{32}(I_h)$ to the antibonding π^* orbit of CO. The HOMO available charge density of this structure shown in Fig. 3 (V) provides

TABLE I. The calculated structural and electronic properties for the interaction of CO molecule with cluster $Au_{32}(I_h)$ and cluster $Au_{32}(C_1)$: binding energy of CO E_b (eV), HOMO-LUMO gap E_g (eV), C–O bond length r(C–O) (Å), and Au–C bond length r(Au–C) (Å).

System	E_b	E_g	r(C–O)	r(Au–C)
		$Au_{32}(I_h)$–CO		
I	0.86	1.45	1.15	1.98
II	0.40	1.26	1.15	2.06
III	0.12	1.54	1.14	···
IV	0.01	1.56	1.14	···
V	−0.08	0.47	1.17	2.19 2.22
		$Au_{32}(C_1)$–CO		
I	1.10	0.29	1.15	1.96
II	1.08	0.46	1.15	1.96
III	1.03	0.85	1.19	2.15 2.16 2.28

an evidence for this charge transfer. It can be seen that considerable part of the HOMO concentrates around CO and two Au atoms, on which CO is bound, showing that CO gains more electrons in this structure of $Au_{32}(I_h)$–CO than its four counterparts. Accompanying with the geometric structure change of the $Au_{32}(I_h)$ cage, its electronic properties also change upon CO adsorption. For instance, the HOMO-LUMO gap of this structure is much narrower, only 0.47 eV.

The amorphous Au_{32} cluster $Au_{32}(C_1)$ has a structure without any symmetry, resulting in many sites available to bind CO to form $Au_{32}(C_1)$–CO. In fact, the present calculations give many stable structures of $Au_{32}(C_1)$–CO. Only the three most stable structures are selected and shown in Fig. 2(b). It can be seen that the behavior of CO on $Au_{32}(C_1)$ is similar to that on $Au_{32}(I_h)$. CO is adsorbed on the on-top sites of $Au_{32}(C_1)$ cluster with C atom attached to Au atom. The ground-state structure (I) and the first isomer structure (II) of $Au_{32}(C_1)$–CO complex are very similar to each other, and the total energy difference between them is only 0.01 eV. In these two structures, CO is bound to a single Au atom, but at different sites. The C–O bond length increases to 1.15 Å, a bond length of CO^-, while the Au–C bond length is 1.96 Å. Therefore, it is suggested that one electron might transfer from Au atom to the π^* orbit of CO, indicating chemical adsorption of CO on $Au_{32}(C_1)$. However, in the third stable structure of $Au_{32}(C_1)$–CO (III), CO is bound to the surface of $Au_{32}(C_1)$ in such a way that three Au–C bonds are formed simultaneously, and the C–O bond is stretched to 1.19 Å. This means that more than one electron transfer from Au atoms to the antibonding π^* orbit of CO. Compared with the highest binding energy of CO in the $Au_{32}(I_h)$–CO complex, 0.86 eV, the binding energy of CO in the $Au_{32}(C_1)$–CO complex is even higher, i.e., 1.09, 1.08, and 1.03 eV, respectively, for the three most stable structures of $Au_{32}(C_1)$–CO shown in Fig. 2(b), indicating that $Au_{32}(I_h)$ is more inert than $Au_{32}(C_1)$ with respect to the interaction with CO.

In summary, present calculation shows that CO can be chemically adsorbed on Au_{32} cluster for both $Au_{32}(I_h)$ and $Au_{32}(C_1)$, but the CO adsorption on $Au_{32}(C_1)$ is stronger than that on $Au_{32}(I_h)$. Accompanying with the chemisorption of CO, electrons transfer from Au_{32} cluster to the antibonding π^* orbit of CO, resulting in the increase of C–O bond length and formation of Au–C bond. $Au_{32}(I_h)$ shows a higher chemical inertness than $Au_{32}(C_1)$. Although CO can be chemically adsorbed on $Au_{32}(I_h)$, the adsorption of CO does not bring out remarkable effects on $Au_{32}(I_h)$. In addition, the five-coordinated sites of $Au_{32}(I_h)$ are the active sites, more favorable for CO adsorption.

B. Interaction between cluster Au_{32} and H_2

The interactions between cluster Au_{32} and H_2 are also investigated in the present work. First, the possible structures of Au_{32}–H_2 complexes are explored. The structures are optimized, and the most stable ones are shown in Fig. 4 for $Au_{32}(I_h)$–H_2 (a) and $Au_{32}(C_1)$–H_2 (b). Their structural and electronic properties, i.e., the binding energy of H_2, HOMO-LUMO gap, and the bond lengths of H–H and Au–H, are listed in Table II. In addition, HOMO charge densities of $Au_{32}(I_h)$–H_2 complexes are calculated and plotted in Fig. 5.

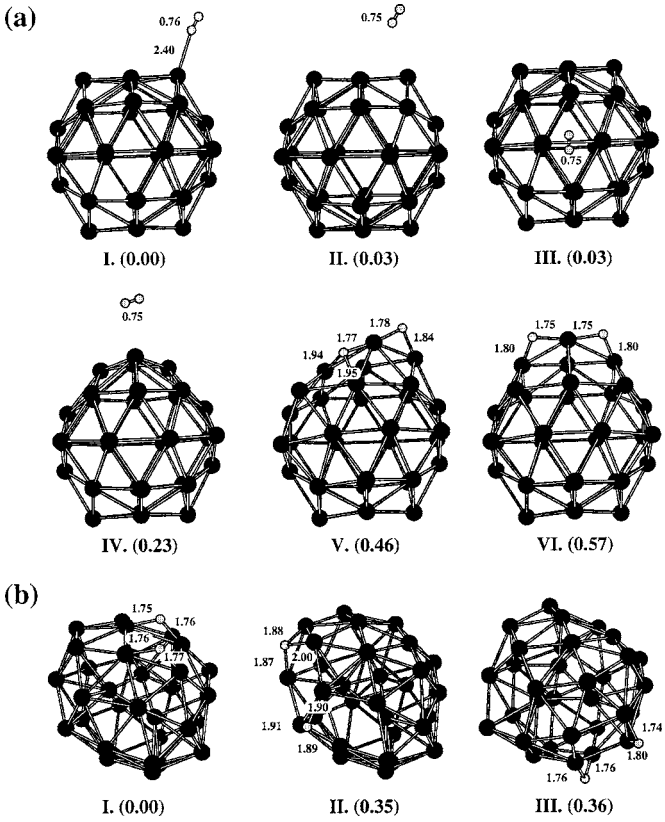

FIG. 4. Structures of Au_{32}–H_2: (a) $Au_{32}(I_h)$–H_2 and (b) $Au_{32}(C_1)$–H_2. The gray balls represent H atoms. The bond lengths of H–H and Au–H are given in Å. What shown in brackets are the relative energies to the total energies of the ground state structures of $Au_{32}(I_h)$–H_2 and $Au_{32}(C_1)$–H_2, respectively, in eV.

For $Au_{32}(I_h)$–H_2, many structures are obtained from the present calculation, only the six most stable ones are shown in Fig. 4(a), according to the sequence of their stability. In the ground state structure of $Au_{32}(I_h)$–H_2 (I), molecule H_2 is adsorbed on the top of the five-coordinated site, forming one

TABLE II. The calculated structural and electronic properties for the interaction of H_2 molecule with cluster $Au_{32}(I_h)$ and cluster $Au_{32}(C_1)$: binding energy of H_2 E_b (eV), HOMO-LUMO gap E_g (eV), H–H bond length r(H–H) (Å), and Au–H bond length r(Au–H) (Å).

System	E_b	E_g	r(H–H)	r(Au–H)
			$Au_{32}(I_h)$–H_2	
I	0.33	1.56	0.76	2.40
II	0.30	1.56	0.75	3.15
III	0.30	1.56	0.75	···
IV	0.10	1.33	0.75	···
V	–0.12	0.77	···	1.77 1.78 1.84 1.94 1.95
VI	–0.24	0.63	···	1.75 1.75 1.80 1.80
			$Au_{32}(C_1)$–H_2	
I	0.98	0.86	···	1.76 1.76 1.77 1.77
II	0.64	0.78	···	1.87 1.88 1.89 1.90 1.91 2.00
III	0.62	0.73	···	1.74 1.76 1.76 1.80

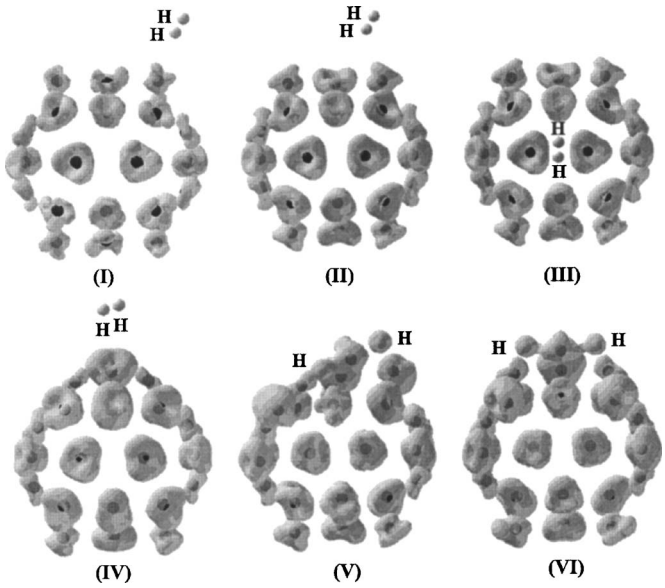

FIG. 5. The highest occupied states (HOMO) of $Au_{32}(I_h)$–H_2 complexes. The plots show equal density surface of 0.04 electrons/Å.

weak Au–H bond, the $Au_{32}(I_h)$ cage keeps almost unchanged, meanwhile the H–H bond length increases to 0.76 Å, 0.01 Å longer than that of a free H_2, 0.75 Å. The interaction of H_2 with $Au_{32}(I_h)$ is weak, with the binding energy of only 0.33 eV. The HOMO charge density shown in Fig. 5 confirms this weak adsorption. Although the HOMO of $Au_{32}(I_h)$ cage is disturbed somehow by H_2 adsorption, it is far away from H_2, indicating no charge transfer from $Au_{32}(I_h)$ to H_2 occurred, i.e., physical adsorption of H_2 on $Au_{32}(I_h)$. Upon H_2 adsorption, the geometric and electronic structures of $Au_{32}(I_h)$ cage experience only neglectable changes; therefore $Au_{32}(I_h)$ keeps its wide HOMO-LUMO gap unchanged, 1.56 eV. The present calculation shows that H_2 is only physically adsorbed on the five-coordinated sites of $Au_{32}(I_h)$, it cannot be adsorbed on the six-coordinated sites at all. This is another evidence to reveal that the five-coordinated sites have higher chemical activity than the six-coordinated sites of $Au_{32}(I_h)$.

H_2 stays on the outer surface of $Au_{32}(I_h)$ cage in the second stable structure of $Au_{32}(I_h)$–H_2 (II), while it stays at the inner center of $Au_{32}(I_h)$ cage in the third stable structure of $Au_{32}(I_h)$–H_2 (III). In these two cases, H_2 keeps its free molecule state with a H–H bond length of 0.75 Å, while $Au_{32}(I_h)$ cages keep their structures unchanged, too. The HOMO densities of these two structures are shown as (II) and (III) in Fig. 5. It is clearly seen that addition of H_2 molecules does not disturb the HOMO distributions of $Au_{32}(I_h)$, and no part of it exists around H_2. This confirms that upon addition of H_2, the wide HOMO-LUMO gaps in these two structures do not change either, but keep the value of 1.56 eV. The binding energy of H_2 in the two structures is calculated to be 0.30 eV, suggesting that H_2 can stay either on the outer surface or at the inner center of the $Au_{32}(I_h)$ cage. Therefore, $Au_{32}(I_h)$ cage can stably store H_2 inside, unlike that of C_{60} cage which destabilizes H_2 staying at its center.[54]

Only weak interaction between $Au_{32}(I_h)$ and H_2 exists in the fourth stable structure of $Au_{32}(I_h)$–H_2 (IV) with a low binding energy of H_2, 0.10 eV, where H_2 keeps its free molecule state. It is shown that adsorption of H_2 leads to part of the structure of $Au_{32}(I_h)$ close to the adsorbed H_2 distorted. The structural distortion of $Au_{32}(I_h)$ causes part of the HOMO close to the adsorption site of H_2 redistributed, while the other part of the HOMO keeps unchanged. However, no part of the HOMO concentrates around the adsorbed H_2. Upon adsorbing H_2 the HOMO-LUMO gap of $Au_{32}(I_h)$ decreases to a slightly narrower value, 1.33 eV. Briefly, adsorption of H_2 does not bring out a remarkable influence to $Au_{32}(I_h)$.

Besides the H_2 molecularly adsorbed structures, the structures of $Au_{32}(I_h)$–H_2, in which H_2 is dissociatively adsorbed, should also be taken into consideration. In the present calculation such kind of structures is also optimized. All the structures, in which the H_2 is dissociatively adsorbed, have higher total energy than those in which the H_2 is molecularly adsorbed, indicating that the latter is more stable. In this paper, only two most stable H_2 dissociatively adsorbed structures of $Au_{32}(I_h)$–H_2 are selected and shown in Fig. 4(a) as (V) and (VI). The binding energy of H_2 is positive in the case of H_2 molecularly adsorbed on $Au_{32}(I_h)$, i.e., the molecular adsorption of H_2 is exothermic; while it is negative in the case of H_2 dissociatively adsorbed on $Au_{32}(I_h)$, i.e., the dissociative adsorption of H_2 is endothermic. Since the dissociation of H_2 needs a fairly high energy, H_2 molecule would rather like not to be adsorbed than dissociatively adsorbed on $Au_{32}(I_h)$. Therefore H_2 can only be molecularly adsorbed on $Au_{32}(I_h)$, and $Au_{32}(I_h)$ shows a high inertness with respect to the interaction with H_2. Previous studies reported that the hydrogenation occurred only at high temperature and under high pressure, though H_2 can be dissociated and adsorbed on small Au_n^+.[10,30] Similar to the case of small Au_n^+, it is proposed that the hydrogenation of $Au_{32}(I_h)$ is very difficult except under special conditions. When H_2 is dissociatively adsorbed on $Au_{32}(I_h)$, each H atom would like to contact with two or three Au atoms, resulting in the $Au_{32}(I_h)$ cage broken and the electronic structures of $Au_{32}(I_h)$ changed. The HOMO charge densities of such kind of structures shown in Fig. 5 indicate that H atoms gain electrons from $Au_{32}(I_h)$, inducing the redistribution of the HOMO of $Au_{32}(I_h)$. In addition, upon dissociative adsorption of H_2 on $Au_{32}(I_h)$, HOMO-LUMO gaps of the clusters decrease remarkably to 0.77 and 0.63 eV for structures (V) and (VI), respectively.

For the amorphous cluster $Au_{32}(C_1)$, the interaction with H_2 leads to only two kinds of stable structures: one is H_2 dissociatively adsorbed on $Au_{32}(C_1)$, and the other is molecular H_2 staying on the outer surface of $Au_{32}(C_1)$ without chemically bonding with $Au_{32}(C_1)$. The present calculations show that the former is more stable than the latter, opposite to the case of $Au_{32}(I_h)$. Figure 4(b) shows the three most stable structures of $Au_{32}(C_1)$–H_2 obtained; in all these three structures, upon adsorption on $Au_{32}(C_1)$ H_2 dissociates to two H atoms, each H atom tends to connect with two or three Au atoms. The binding energy of H_2 of $Au_{32}(C_1)$–H_2 is positive and much more than those of $Au_{32}(I_h)$–H_2, it is 0.98, 0.64, and 0.62 eV for he three most stable structures of

$Au_{32}(C_1)-H_2$, respectively, by comparison it is only 0.33 eV for the most stable $Au_{32}(I_h)-H_2$. This shows that during H_2 desorption on $Au_{32}(C_1)$ enough energy is released to overcome the high energy barrier of H_2 dissociation. Therefore molecular H_2 can be dissociatively chemisorbed on $Au_{32}(C_1)$. It illustrates that $Au_{32}(I_h)$ has higher chemical inertness than $Au_{32}(C_1)$ with respect to the interaction with H_2.

In summary, H_2 can only be physically adsorbed on the five-coordinated sites of $Au_{32}(I_h)$, while it can be dissociatively chemisorbed on $Au_{32}(C_1)$. $Au_{32}(I_h)$ has a higher chemical inertness than $Au_{32}(C_1)$ with respect to the interaction with H_2, and it almost keeps its original state unchanged in this interaction.

C. Interaction between cluster Au_{32} and O_2

The interaction of Au_{32} cluster with O_2 would be more complicated than the interaction of Au_{32} clusters with CO and H_2 because of the many adsorption mechanisms involved for O_2. These mechanisms are accompanied by a different number of electrons transferred from Au clusters to the antibonding π^* orbit of O_2, e.g., (a) physical adsorption corresponding to zero electron transfer; (b) molecular chemisorption to yield superoxide, O_2^-, corresponding to one electron transfer; (c) molecular chemisorption to yield peroxide, O_2^{2-}, corresponding to two electron transfer; and (d) dissociative chemisorption to yield two oxide adsorbates corresponding to four electron transfer. In addition, the properties of O_2 molecule are also more complicated because of its two kinds of spin states: ground state [spin-triplet, O_2(triplet)] and excited state [spin-singlet, O_2(singlet)]. Therefore, in order to study the interaction of Au_{32} clusters with O_2 molecules, both spin polarized and nonpolarized calculations, for spin-triplet O_2(triplet) and spin-singlet O_2(singlet), respectively, should be carried out.

First, consider the spin polarized calculations. Figure 6 displays the most stable structures of $Au_{32}-O_2$(triplet) complexes obtained for $Au_{32}(I_h)-O_2$(triplet) (a) and $Au_{32}(C_1)-O_2$(triplet) (b). Their structural and electronic properties, i.e., the binding energy of O_2(triplet), HOMO-LUMO gap, magnetic moment, and the bond lengths of O–O and Au–O, are listed in Table III. In addition, the HOMO charge densities of $Au_{32}(I_h)-O_2$(triplet) complexes are plotted in Fig. 7.

Similar to $Au_{32}-H_2$ complexes, both molecular adsorption and dissociative adsorption of O_2 should be considered for $Au_{32}-O_2$ complexes. Therefore, a great number of possible structures of $Au_{32}-O_2$ complexes are obtained. Here only six most stable structures of $Au_{32}(I_h)-O_2$(triplet) and three most stable structures of $Au_{32}(C_1)-O_2$(triplet) are selected and shown in Fig. 6.

In the ground state structure of $Au_{32}(I_h)-O_2$(triplet) (I), upon adsorption on $Au_{32}(I_h)$ molecular O_2 is dissociated symmetrically into two O atoms, resulting in the $Au_{32}(I_h)$ cage broken. The dissociative chemisorption of O_2 not only breaks the geometric structure of the $Au_{32}(I_h)$ cage but also changes its electronic property. The HOMO charge density [see (I) in Fig. 7] shows that the HOMO mostly concentrates around the O atoms and those Au atoms nearby, indicating

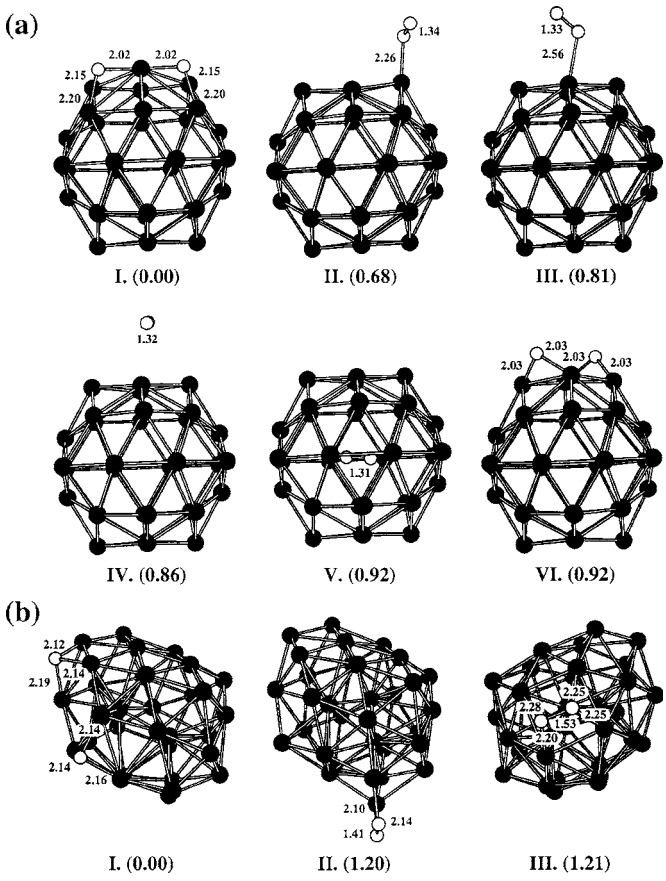

FIG. 6. Structures of $Au_{32}-O_2$(triplet): (a) $Au_{32}(I_h)-O_2$(triplet) and (b) $Au_{32}(C_1)-O_2$(triplet). The white balls represent O atoms. The bond lengths of O–O and Au–O are given in Å. What shown in brackets are the relative energies to the total energy of the ground state structures of $Au_{32}(I_h)-O_2$(triplet) and $Au_{32}(C_1)-O_2$(triplet), respectively, in eV.

the electron transfer from $Au_{32}(I_h)$ to the antibonding π^* orbit of O_2, leading to the O–O bond broken and the Au–O bond formed. Due to the interaction of $Au_{32}(I_h)$ with O_2, its HOMO-LUMO gap remarkably decreases to 0.34 eV. Compared to other structures of $Au_{32}(I_h)-O_2$(triplet), this ground state structure of O_2 dissociative chemisorption is energeti-

TABLE III. The calculated structural and electronic properties for the interaction of O_2(triplet) molecule with cluster $Au_{32}(I_h)$ and cluster $Au_{32}(C_1)$: binding energy of O_2(triplet) E_b (eV), HOMO-LUMO gap E_g (eV), magnetic moment mag(μ_B), O–O bond length r(O–O) (Å), and Au–O bond length r(Au–O) (Å).

System	E_b	E_g	mag	r(O–O)	r(Au–O)
			$Au_{32}(I_h)-O_2$(triplet)		
I	1.16	0.34	0	···	2.02 2.02 2.15 2.15 2.20 2.20
II	0.48	0.47	2	1.34	2.26
III	0.35	0.62	2	1.33	2.56
IV	0.30	0.51	2	1.32	···
V	0.24	0.52	2	1.32	···
VI	0.24	0.40	0	···	2.03 2.03 2.03 2.03
			$Au_{32}(C_1)-O_2$(triplet)		
I	2.06	0.49	0	···	2.12 2.14 2.14 2.14 2.16 2.19
II	0.86	0.09	0	1.41	2.10 2.14
III	0.84	0.37	0	1.53	2.20 2.25 2.25 2.28

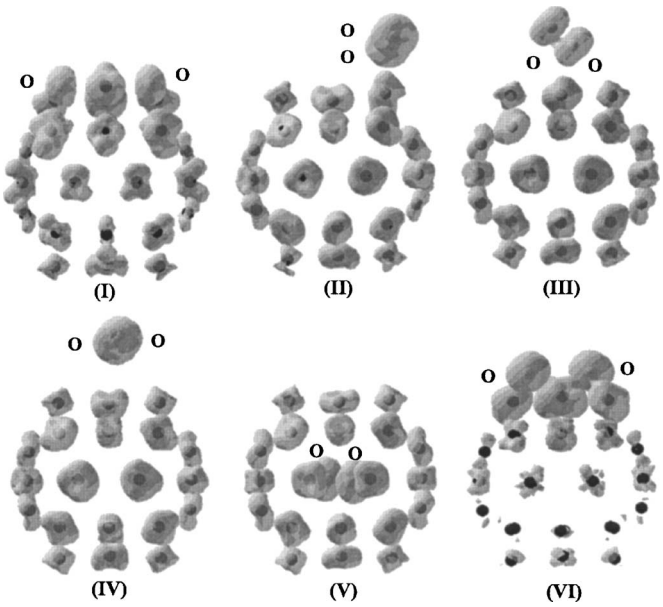

FIG. 7. The highest occupied states (HOMO) of $Au_{32}(I_h)-O_2$(triplet) complexes. The plots show equal density surface of 0.04 electrons/Å.

cally most favorable, which has the highest binding energy of O_2(triplet), 1.16 eV. However, as both the dissociation of O_2(triplet) and break of $Au_{32}(I_h)$ need to overcome high energy barriers, some special conditions must be available to promote this interaction. Similar to the present calculations, previous theoretical and experimental studies reported that dissociative adsorption of O_2 on C_{60} cage, accompanied with the cage broken, only happened at the temperatures higher than 200 °C.[55,56]

O_2 is molecularly adsorbed on the top of the five-coordinated site of $Au_{32}(I_h)$ in the second stable structure of $Au_{32}(I_h)-O_2$(triplet) (II) and on the top of the six-coordinated site of $Au_{32}(I_h)$ in the third stable structure (III), only one Au–O bond formed in both structures. The energy difference of these two structures is 0.23 eV. This is a more evidence to show that the five-coordinated sites are more active than the six-coordinated sites of $Au_{32}(I_h)$. The present calculation shows that, for these two structures, adsorption of O_2(triplet) does not make any noticeable change of the $Au_{32}(I_h)$ structure, the O–O bond length only slightly increases to 1.34 and 1.33 Å, respectively, 0.03 and 0.02 Å longer han that of a free O_2, 1.31 Å. It is interesting to notice that the binding energies of O_2(triplet) for these two structures are only 0.48 and 0.35 eV, respectively, much smaller than that for the ground state structure. This suggests that no electron is transferred from $Au_{32}(I_h)$ to O_2 in these two structures, i.e., O_2(triplet) is only physically adsorbed on $Au_{32}(I_h)$. The HOMO charge densities of these two structures are plotted in Fig. 7 [(II) and (III)], supporting the above analysis. The figure shows only slight distortion of the HOMO distribution of $Au_{32}(I_h)$ cage, i.e., the HOMO around the Au atom binding the O_2 molecules spreads a little towards the O_2 but without any charge transfer between Au and O. Though O_2(triplet) is only physically adsorbed in the second and third stable structures of $Au_{32}(I_h)-O_2$(triplet), they are obviously different from the ground state structure of $Au_{32}(I_h)-O_2$(triplet), their HOMO-LUMO gap also decreases remarkably. The gaps of the second and the third stable structures of $Au_{32}(I_h)-O_2$(triplet) are 0.47 and 0.62 eV, respectively.

In the fourth and the fifth stable structures of $Au_{32}(I_h)-O_2$(triplet) [(IV) and (V) in Fig. 6], O_2 molecule stays on the outer surface and at the inner center of $Au_{32}(I_h)$ cage, respectively. O_2 molecules keep in free molecular state, and $Au_{32}(I_h)$ cages keep their original geometric structures unchanged, too. Examination of the HOMO charge densities [(IV) and (V) in Fig. 7], shows no change of the HOMO of both $Au_{32}(I_h)$ and O_2 occurred, indicating no charge transfer between them. The weak interaction of $Au_{32}(I_h)$ and O_2 corresponds to very small binding energies of O_2 for these two structures, only 0.30 and 0.24 eV, respectively. Even though, the adsorption of O_2 does influence $Au_{32}(I_h)$ somehow for both fourth and fifth stable clusters. For example, the wide HOMO-LUMO gap of $Au_{32}(I_h)$ decreases to 0.51 and 0.52 eV, respectively.

In the sixth stable structure of $Au_{32}(I_h)-O_2$(triplet) complex, though O_2 molecule is dissociatively adsorbed on $Au_{32}(I_h)$, the $Au_{32}(I_h)$ cage is only slightly distorted. This is different from the ground state structure of $Au_{32}(I_h)-O_2$(triplet), in which the $Au_{32}(I_h)$ cage is broken. In this structure, O atoms are located at the bridge sites between five-coordinated Au atom and six-coordinated Au atom. Dissociative adsorption of O_2 should be accompanied with charge transfer, which is proved by the HOMO charge density shown in Fig. 7 (VI). It can be seen that the HOMO mostly concentrates around O atoms and those Au atoms nearby. Therefore O_2 gains electrons from $Au_{32}(I_h)$ and the electrons occupy the π^* orbit of O_2, which makes O_2 molecule dissociatively chemisorbed on $Au_{32}(I_h)$. Although O_2 molecule is dissociated and chemisorbed on $Au_{32}(I_h)$ in both ground state structure and sixth stable structure, the binding energies of O_2(triplet) are very different, which are 1.16 and 0.24 eV, respectively. Energy difference comes from the structural difference: O_2 dissociation and chemisorption make $Au_{32}(I_h)$ cage of the ground state structure broken but $Au_{32}(I_h)$ cage of the sixth stable structure only slightly distorted. This shows that O_2 dissociative adsorption on $Au_{32}(I_h)$ should favor the structural break of $Au_{32}(I_h)$.

Although the molecular chemisorption of O_2 can also be found in some isomers of $Au_{32}(I_h)-O_2$(triplet) and O_2 appears in O_2^- or O_2^{2-} state, their binding energy of O_2(triplet) is negative and those isomers are unstable. Therefore for spin-triplet O_2, superoxide or peroxide cannot be formed through the interaction with $Au_{32}(I_h)$.

For amorphous $Au_{32}(C_1)-O_2$(triplet) complexes, both O_2 dissociatively chemisorbed and molecularly chemisorbed structures are found. Figure 6(b) shows three most stable ones of them. Similar to $Au_{32}(I_h)-O_2$(triplet), O_2 is dissociatively adsorbed in the ground state structure of $Au_{32}(C_1)-O_2$(triplet) [(I) of Fig. 6(b)] and gets four electrons from $Au_{32}(C_1)$. However, in the second and third stable structures [(II) and (III) of Fig. 6(b)], O_2 molecules are molecularly chemisorbed on different sites and the O–O bond lengths increase to 1.41 and 1.53 Å, respectively. The value of 1.41 Å is close to the bond length of O_2^-, and the value of

1.53 Å is close to the bond length of O_2^{2-}. Therefore O_2 forms superoxide state and gets one electron from $Au_{32}(C_1)$ in the second stable structure, while O_2 forms peroxide state and obtains two electrons from $Au_{32}(C_1)$ in the third stable structure. The binding energy of O_2(triplet) in $Au_{32}(C_1)-O_2$(triplet) is much higher than in $Au_{32}(I_h)-O_2$(triplet). For example, the binding energy of O_2(triplet) for the ground state structure of $Au_{32}(C_1)-O_2$(triplet) is 2.06 eV, 0.90 eV higher than that for the ground state structure of $Au_{32}(I_h)-O_2$(triplet). Meanwhile, O_2 can be molecularly chemisorbed on $Au_{32}(C_1)$, but can only be physically adsorbed on $Au_{32}(I_h)$. Therefore $Au_{32}(I_h)$ is more inert than with respect to the interaction with O_2(triplet).

It can be seen from the spin polarized calculations that the corresponding ground state structures are that, in which O_2 is dissociatively chemisorbed for both $Au_{32}(I_h)-O_2$(triplet) and $Au_{32}(C_1)-O_2$(triplet). Although the O_2 dissociative chemisorption is energetically favorable in $Au_{32}(I_h)-O_2$(triplet), it is suggested that the formation of this structure should require some special condition, since both the dissociation of O_2 and break of $Au_{32}(I_h)$ need to overcome high barriers. Except the dissociative chemisorption of O_2, no stable molecular chemisorption of O_2 is found in the $Au_{32}(I_h)-O_2$(triplet), and O_2 is only physically adsorbed on $Au_{32}(I_h)$ or freely stays outside or inside the $Au_{32}(I_h)$. However, for $Au_{32}(C_1)-O_2$(triplet), in addition to the dissociative chemisorption of O_2, the molecular chemisorption of O_2 is also favorable, and both superoxide and peroxide can be found. Both dissociative chemisorption and molecular chemisorption of O_2 are accompanied with the charge transfer from cluster Au_{32} to O_2, resulting in the transition of O_2 from spin triplet to spin singlet. Compared to $Au_{32}(C_1)$, $Au_{32}(I_h)$ is more chemically inert with respect to the interaction with spin-triplet O_2. Besides, the interaction with spin-triplet O_2 leads to the HOMO-LUMO gap of $Au_{32}(I_h)$ decreased.

Next, let us discuss the spin nonpolarized calculations. Figure 8 displays the most stable structures of $Au_{32}(I_h)-O_2$(singlet) (a) and $Au_{32}(C_1)-O_2$(singlet) (b). Their structural and electronic properties, i.e., the binding energy of O_2(singlet), HOMO-LUMO gap, and the bond lengths of O–O and Au–O, are listed in Table IV. In addition, HOMO charge densities of $Au_{32}(I_h)-O_2$(singlet) complexes are plotted in Fig. 9.

The six most stable structures of $Au_{32}(I_h)-O_2$(singlet) are shown in Fig. 8(a). The results of the spin nonpolarized calculations show that in all the five most stable structures of $Au_{32}(I_h)-O_2$(singlet) O_2 is dissociatively chemisorbed, except the sixth one [(VI) in Fig. 8(a)]. The ground state structure of $Au_{32}(I_h)-O_2$(singlet) (I) is almost as the same as the ground state structure of $Au_{32}(I_h)-O_2$(triplet). The binding energies of O_2(singlet) and O_2(triplet) are 2.06 and 1.16 eV, respectively; the difference between them, 0.9 eV, is equal to the difference between the total free energy of spin-singlet O_2 and that of spin-triplet O_2. Because the magnetic moment of this structure is $0\mu_B$ and the dissociation of O_2 induces the transition of O_2 from spin triplet to spin singlet, the spin polarized calculations and spin nonpolarized calculations lead to the same results. In the second stable structure of $Au_{32}(I_h)-O_2$(singlet) [(II) in Fig. 8(a)], O_2 is dissociated and chemisorbed on the outer surface of $Au_{32}(I_h)$, accompanying with the $Au_{32}(I_h)$ cage broken, too. In the third, fourth, and fifth stable structures [(III), (IV), and (V) in Fig. 8(a)], although O_2 molecules are dissociated, the $Au_{32}(I_h)$ cages keep unbroken but slightly distorted. It is found that the binding energies of O_2(singlet) for the two most stable structures of

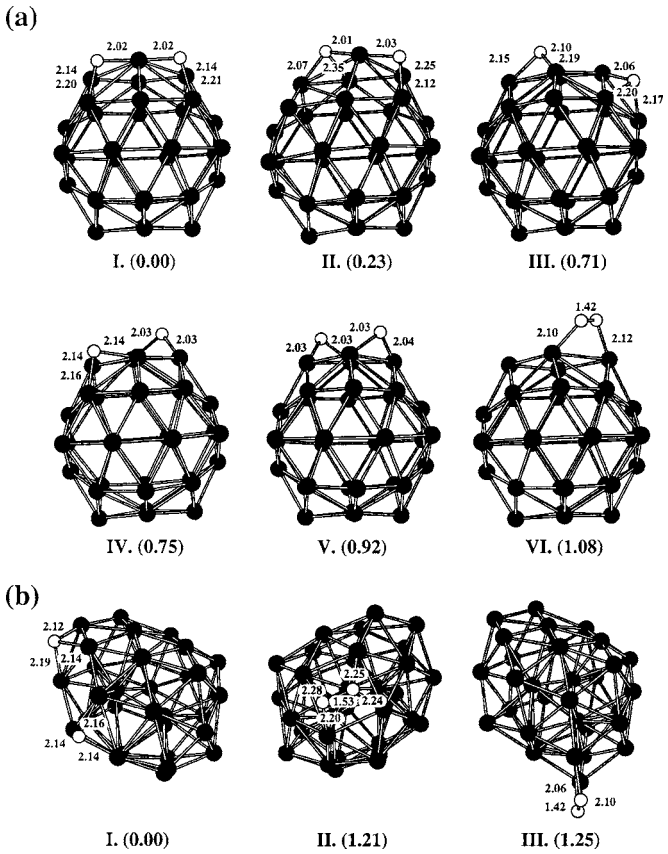

FIG. 8. Structures of $Au_{32}-O_2$ (singlet): (a) $Au_{32}(I_h)-O_2$ (singlet) and (b) $Au_{32}(C_1)-O_2$ (singlet). The white balls represent O atoms. The bond lengths of O–O and Au–O are given in Å. What shown in brackets are the relative energies to the total energy of the ground state structures of $Au_{32}(I_h)-O_2$ (singlet) and $Au_{32}(C_1)-O_2$ (singlet), respectively, in eV.

TABLE IV. The calculated structural and electronic properties for the interaction of O_2(singlet) molecule with cluster $Au_{32}(I_h)$ and cluster $Au_{32}(C_1)$: binding energy of O_2(singlet) E_b (eV), HOMO-LUMO gap E_g (eV), O–O bond length r(O–O) (Å), and Au–O bond length r(Au–O) (Å).

System	E_b	E_g	r(O–O)	r(Au–O)
		$Au_{32}(I_h)-O_2$(singlet)		
I	2.20	0.35	···	2.02 2.02 2.20 2.21 2.14 2.14
II	1.97	0.42	···	2.01 2.03 2.07 2.12 2.25 2.35
III	1.49	0.37	···	2.07 2.10 2.15 2.17 2.19 2.20
IV	1.45	0.41	···	2.03 2.03 2.14 2.14 2.16
V	1.28	0.45	···	2.03 2.03 2.03 2.04
VI	1.12	0.14	1.42	2.10 2.12
		$Au_{32}(C_1)-O_2$(singlet)		
I	3.09	0.50	···	2.12 2.14 2.14 2.14 2.16 2.19
II	1.88	0.37	1.53	2.20 2.25 2.25 2.28
III	1.84	0.23	1.42	2.07 2.10

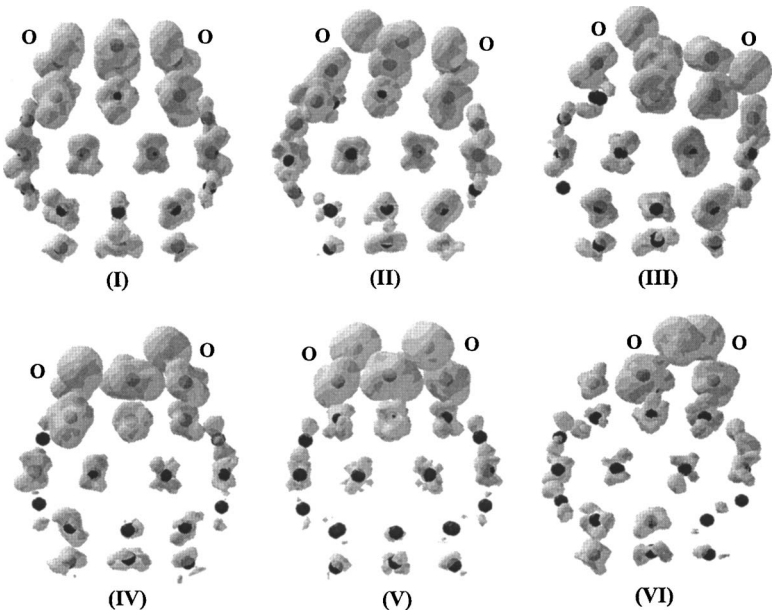

FIG. 9. The highest occupied states (HOMO) of $Au_{32}(I_h)-O_2$ (singlet) complexes. The plots show equal density surface of 0.04 electrons/Å.

$Au_{32}(I_h)-O_2$(singlet) [(I) and (II)] are much higher than those for the other three structures [(III), (IV), and (V)]. The reason is that the break of $Au_{32}(I_h)$ cage would make the dissociative adsorption of O_2 more stable. Moreover the HOMO charge densities (Fig. 9) show that for all the first five structures considered the HOMO is mostly distributed around O atoms and those Au atoms binding the O atoms, corresponding to that O_2 is dissociatively adsorbed on $Au_{32}(I_h)$, no matter whether the cage is broken or not. This means that the dissociative adsorption of O_2 is accompanied with the charge transfer from $Au_{32}(I_h)$ to O_2. In the sixth stable structure of $Au_{32}(I_h)-O_2$(singlet) [(VI) in Fig. 8(a)], O_2 is molecularly chemisorbed on $Au_{32}(I_h)$ and bound on the bridge site between five-coordinated Au atom and six-coordinated Au atom with O–O bond length increased to 1.42 Å, which is close to the value of O_2^-. This suggests that electrons transfer from $Au_{32}(I_h)$ to O_2, leading to the formation of superoxide. The HOMO charge density supports this analysis. The HOMO distribution shown in (VI) of Fig. 9 shows that a considerable part concentrates around O_2 and those Au atoms nearby. For these six structures of $Au_{32}(I_h)-O_2$(singlet), HOMO-LUMO gaps are all narrow, i.e., the spin nonpolarized calculations also indicate that the interaction with O_2 causes the energy gap of $Au_{32}(I_h)$ narrowed.

As to the amorphous clusters, three most stable structures of $Au_{32}(C_1)-O_2$(singlet) are shown in Fig. 8(b). The ground state structure of $Au_{32}(C_1)-O_2$(singlet) [(I) in Fig. 8(b)] is almost as the same as the ground state structure of $Au_{32}(C_1)-O_2$(triplet) [(I) in Fig. 6(b)], in which O_2 is dissociatively chemisorbed on $Au_{32}(C_1)$. This is because from the pin polarized calculation, the magnetic moment of this structure is $0\mu_B$, i.e., O_2 is in spin singlet in this structure. The second stable structure of $Au_{32}(C_1)-O_2$(singlet) [(II) in Fig. 8(b)] is almost as the same as the third stable structure of $Au_{32}(C_1)-O_2$(triplet) [(III) in Fig. 6(b)], while the third stable structure of $Au_{32}(C_1)-O_2$(singlet) [(III) in Fig. 8(b)] is almost as the same as the second stable structure of $Au_{32}(C_1)-O_2$(triplet) [(II) in Fig. 6(b)]. This means that from the spin nonpolarized calculations the peroxide is energetically more favorable than the superoxide. For spin-singlet O_2, because it is in the excited state, it can trap electrons more easily than spin-triplet O_2. Either in the present spin polarized calculations or in the spin nonpolarized calculation, the energy of the second stable structure is approximately equal to that of the third one. Similar to the results of the spin polarized calculations, from the spin nonpolarized calculations the binding energy of O_2(singlet) of $Au_{32}(C_1)-O_2$(singlet) is higher than that of $Au_{32}(I_h)-O_2$(singlet), indicating the high chemical inertness of $Au_{32}(I_h)$.

Briefly, the present spin nonpolarized calculations show that dissociative chemisorption of O_2 is most favorable for both $Au_{32}(I_h)$ and $Au_{32}(C_1)$. For $Au_{32}(I_h)-O_2$(singlet), of all the six most stable structures five are that, in each of them O_2 is dissociatively chemisorbed, except one is that, in which O_2 is molecularly chemisorbed. For $Au_{32}(C_1)-O_2$(singlet), the structure in which O_2 is dissociatively adsorbed is most stable, the peroxide is the second stable structure and the superoxide is the third stable structure, i.e., the more electrons transferred from $Au_{32}(C_1)$ to O_2, the more stable the structure will be. With respect to the interaction with spin-singlet O_2, $Au_{32}(I_h)$ also exhibits higher chemical inertness than $Au_{32}(C_1)$. Interaction with O_2 decreases remarkably the HOMO-LUMO gap of $Au_{32}(I_h)$.

IV. CONCLUSIONS

In conclusion, first-principles calculations have been carried out on the interactions of $Au_{32}(I_h)$ and $Au_{32}(C_1)$ with CO, H_2, and O_2.

CO can be chemically adsorbed on $Au_{32}(I_h)$ and $Au_{32}(C_1)$, but it is bound more strongly on $Au_{32}(C_1)$ than on $Au_{32}(I_h)$. Accompanied with the chemisorption of CO, electrons transfer from cluster Au_{32} to the antibonding π^* orbit of CO, resulting in the C–O bond length increased and the

Au–C bond formed. The chemisorption of CO exerts only a slight influence on $Au_{32}(I_h)$ for both geometric and electronic properties. The five-coordinated sites of $Au_{32}(I_h)$ are the active sites, and CO favors more to be adsorbed on these sites. H_2 can only be physically adsorbed on the five-coordinated sites of $Au_{32}(I_h)$, while it can be dissociatively chemisorbed on $Au_{32}(C_1)$. The physical adsorption of H_2 almost does not affect the structural and electronic properties of $Au_{32}(I_h)$. From both the present spin polarized and spin nonpolarized calculations, the ground state structures of both $Au_{32}(I_h)-O_2$ and $Au_{32}(C_1)-O_2$ are O_2 dissociatively chemisorbed structures and they are very similar to each other, because the chemisorption of O_2 is accompanied with the charge transfer from Au cluster to O_2 and the transition of O_2 from spin triplet to spin singlet. For $Au_{32}(I_h)$, because the break of $Au_{32}(I_h)$ cage and the chemisorption of O_2 both need to overcome high barriers, the formation of the O_2 dissociatively chemisorbed structure of $Au_{32}(I_h)-O_2$(triplet) must be under some special conditions. Otherwise, spin-triplet O_2 only prefers to be physically adsorbed on $Au_{32}(I_h)$; therefore the spin polarized calculations show no stable O_2 molecularly chemisorbed structure of $Au_{32}(I_h)-O_2$(triplet) existing. For $Au_{32}(C_1)$, both spin polarized calculations and spin nonpolarized calculations show that dissociative O_2 chemisorption on $Au_{32}(C_1)$ is more favorable than molecular chemisorption. In summary, for all three small molecules considered, i.e., CO, H_2, and O_2, their interaction with $Au_{32}(C_1)$ is stronger than that with $Au_{32}(I_h)$. Therefore, $Au_{32}(I_h)$ exhibits higher chemical inertness with respect to the interaction with small molecules, CO, H_2, and O_2.

ACKNOWLEDGMENTS

The authors would like to thank Professor P. Jiang for a critical reading of the manuscript. This work is supported by the National Science Foundation of China and the National Basic Research Program. One of the authors (X.G.G) is also supported by the Shanghai Science and Technology Foundation. The computation is performed in the Supercomputer Center of Shanghai, the Supercomputer Center of Fudan University and CCS, HFCAS.

[1] G. Schmid, Chem. Rev. (Washington, D.C.) **92**, 1709 (1992).
[2] A. P. Alivisatos, Science **271**, 933 (1996).
[3] M. Valden, X. Lai, and D. W. Goodman, Science **281**, 1647 (1998); D. C. Meier and D. W. Goodman, J. Am. Chem. Soc. **126**, 1892 (2004).
[4] M. Haruta, S. Tsubota, T. Kobayashi, H. Kageyama, M. J. Genet, and B. Delmon, J. Catal. **144**, 175 (1993); M. Okumura, J. M. Coronado, J. Soria, M. Haruta, and J. C. Conesa, *ibid.* **203**, 168 (2001).
[5] F. Boccuzzi, A. Chiorino, M. Manzoli, and M. Haruta, J. Catal. **202**, 256 (2001); R. J. H. Grisel, and B. E. Nieuwenhuys, *ibid.* **199**, 48 (2001); M. M. Schubert, S. Hackenberg, A. C. van Veen, M. Muhler, V. Plzak, and R. J. Behm, *ibid.* **197**, 113 (2001).
[6] M. Haruta, Catal. Today **36**, 153 (1997); G. Mul, A. Zwijnenburg, B. van der Linden, M. Makkee, and J. A. Moulijn, J. Catal. **201**, 128 (2001).
[7] J. F. Jia, K. Haraki, J. N. Kondo, K. Domen, and K. Tamaru, J. Phys. Chem. B **104**, 11153 (2000).
[8] A. Sárkány and Z. Révay, Appl. Catal., A **243**, 347 (2003).
[9] C. Mohr, H. Hofmeister, J. Radnik, and P. Claus, J. Am. Chem. Soc. **125**, 1905 (2003).
[10] D. M. Cox, R. O. Brickman, K. Greegan, and A. Kaldor, Z. Phys. D: At., Mol. Clusters **19**, 353 (1991); D. M. Cox, R. O. Brickman, K. Greegan, and A. Kaldor, Mater. Res. Soc. Symp. Proc. **206**, 43 (1991).
[11] T. H. Lee and K. M. Ervin, J. Phys. Chem. **98**, 10023 (1994).
[12] B. E. Salisbury, W. T. Wallace, and R. L. Whetten, Chem. Phys. **262**, 131 (2000); W. T. Wallace and R. L. Whetten, J. Am. Chem. Soc. **124**, 7499 (2002).
[13] J. Hagen, L. D. Socaciu, M. Elijazyfer, U. Heiz, T. M. Bernhardt, and L. Woste, Phys. Chem. Chem. Phys. **4**, 1707 (2002).
[14] D. Stolcic, M. Fischer, G. Ganteför, Y. D. Kim, Q. Sun, and P. Jena, J. Am. Chem. Soc. **125**, 2848 (2003).
[15] Y. D. Kim, M. Fischer, and G. Ganteför, Chem. Phys. Lett. **377**, 170 (2003).
[16] G. Mills, M. S. Gordon, and H. Metiu, Chem. Phys. Lett. **359**, 493 (2002); S. A. Varganov, R. M. Olson, M. S. Gordon, and H. Metiu, J. Chem. Phys. **119**, 2531 (2003).
[17] B. Yoon, H. Häkkinen, and U. Landman, J. Phys. Chem. A **107**, 4066 (2003).
[18] Q. Sun, P. Jena, Y. D. Kim, M. Fischer, and G. Ganteför, J. Chem. Phys. **120**, 6510 (2004).
[19] X. Ding, Z. Li, J. Yang, J. G. Hou, and Q. Zhu, J. Chem. Phys. **120**, 9594 (2004).
[20] X. Wu, L. Senapati, S. K. Nayak, A. Selloni, and M. Hajaligol, J. Chem. Phys. **117**, 4010 (2002).
[21] M. Neumaier, F. Weigend, O. Hampe, and M. M. Kappes, J. Chem. Phys. **122**, 104702 (2005).
[22] L. Jiang and Q. Xu, J. Phys. Chem. A **109**, 1026 (2005).
[23] E. M. Fernández, P. Ordejón, and L. C. Balbás, Chem. Phys. Lett. **408**, 252 (2005).
[24] H.-J. Zhai and L.-S. Wang, J. Chem. Phys. **122**, 051101 (2005).
[25] H. Häkkinen and U. Landman, J. Am. Chem. Soc. **123**, 9704 (2001); L. D. Socaciu, J. Hagen, T. M. Bernhardt, L. Wöste, U. Heiz, H. Häkkinen, and U. Landman, *ibid.* **125**, 10437 (2003).
[26] W. T. Wallace and R. L. Whetten, J. Am. Chem. Soc. **124**, 7499 (2002).
[27] N. Lopez and J. K. Nørskov, J. Am. Chem. Soc. **124**, 11262 (2002).
[28] M. L. Kimble, A. W. Castleman, Jr., R. Mitrić, C. Bürgel, and V. Bonačić-Koutecký, J. Am. Chem. Soc. **126**, 2526 (2004).
[29] D. W. Yuan and Z. Zeng, J. Chem. Phys. **120**, 6574 (2004).
[30] K. Sugawara, F. Sobott, and A. B. Vakhtin, J. Chem. Phys. **118**, 7808 (2003).
[31] S. A. Varganov, R. M. Olson, M. S. Gordon, G. Mills, and H. Metiu, J. Chem. Phys. **120**, 5169 (2004).
[32] A. Sanchez, S. Abbet, U. Heiz, W.-D. Schneider, H. Häkkinen, R. N. Barnett, and U. Landman, J. Phys. Chem. A **103**, 9573 (1999); H. Häkkinen, S. Abbet, A. Sanchez, U. Heiz, and U. Landman, Angew. Chem., Int. Ed. **42**, 1297 (2003); B. Yoon, H. Häkkinen, U. Landman, A. S. Wörz, J.-M. Antonietti, S. Abbet, K. Judai, and U. Heiz, Science **307**, 403 (2005).
[33] Z.-P. Liu, X.-Q. Gong, J. Kohanoff, C. Sanchez, and P. Hu, Phys. Rev. Lett. **91**, 266102 (2003).
[34] L. M. Molina and B. Hammer, Phys. Rev. Lett. **90**, 206102 (2003).
[35] S. Arrii, F. Morfin, A. J. Renouprez, and J. L. Rousset, J. Am. Chem. Soc. **126**, 1199 (2004).
[36] T. S. Kim, J. D. Stiehl, C. T. Reeves, R. J. Meyer, and C. B. Mullins, J. Am. Chem. Soc. **125**, 2018 (2003).
[37] H. Häkkien, M. Moseler, and U. Landman, Phys. Rev. Lett. **89**, 033401 (2002); H. Häkkien, B. Yoon, U. Landman, X. Li, H.-J. Zhai, and L.-S. Wang, J. Phys. Chem. A **107**, 6168 (2003).
[38] F. Furche, R. Ahlrichs, P. Weis, C. Jacob, S. Gilb, T. Bierweiler, and M. M. Kappes, J. Chem. Phys. **117**, 6982 (2002); S. Gilb, P. Weis, F. Furche, R. Ahlrichs, and M. M. Kappes, *ibid.* **116**, 4094 (2002).
[39] J. Li, X. Li, H.-J. Zhai, and L.-S. Wang, Science **299**, 864 (2003).
[40] H.-G. Boyen, G. Kästle, F. Weigl *et al.*, Science **297**, 1533 (2002).
[41] X. Gu, M. Ji, S. H. Wei, and X. G. Gong, Phys. Rev. B **70**, 205401 (2004).
[42] M. Ji, X. Gu, X. Li, X. G. Gong, J. Li, and L.-S. Wang, Angew. Chem., Int. Ed. **44**, 7119 (2005).
[43] P. Hohenberg and W. Kohn, Phys. Rev. **136**, B864 (1964); W. Kohn and L. J. Sham, Phys. Rev. **140**, A1133 (1965).
[44] R. O. Jones and O. Gunnarsson, Rev. Mod. Phys. **61**, 689 (1989).
[45] R. Car and M. Parrinello, Phys. Rev. Lett. **55**, 2471 (1985).
[46] M. C. Payne, M. P. Teter, D. C. Allan, T. A. Arias, and J. D. Joannopoulos, Rev. Mod. Phys. **64**, 1045 (1992).
[47] Y. Wang and J. P. Pedew, Phys. Rev. B **44**, 13298 (1991).
[48] J. P. Pedew, J. A. Chevary, S. H. Vosko, K. A. Jackson, M. R. Pederson, D. J. Singh, and C. Fiolhais, Phys. Rev. B **46**, 6671 (1992).
[49] G. Kresse and J. Furthmüller, Phys. Rev. B **54**, 11169 (1996); Comput.

Mater. Sci. **6**, 15 (1996).
[50] P. E. Blöchl, Phys. Rev. B **50**, 17953 (1994).
[51] G. Kresse and D. Joubert, Phys. Rev. B **59**, 1758 (1999).
[52] M. P. Teter, M. C. Payne, and D. C. Allan, Phys. Rev. B **40**, 12255 (1989).
[53] G. A. Somorjai, *Introduction to Surface Chemistry and Catalysis* (Wiley, New York, 1994).
[54] J. Cioslowski, J. Am. Chem. Soc. **113**, 4139 (1991).
[55] A. M. Vassallo, L. S. K. Pang, P. A. Cole-Clarke, and M. A. Wilson, J. Am. Chem. Soc. **113**, 7820 (1991).
[56] H. S. Chen, A. R. Kortan, R. C. Haddon, and D. A. Fleming, J. Phys. Chem. **96**, 1016 (1992).